Sensory transmission in cerebellar granule cells relies on similarly coded mossy fiber inputs

Fredrik Bengtsson[a] and Henrik Jörntell[a,b,1]

[a]Section for Neurophysiology and [b]Neuronano Research Center, BMC F10, Tornavägen 10, SE-221 84 Lund, Sweden

Edited by Masao Ito, RIKEN, Wako, Japan, and approved December 10, 2008 (received for review September 1, 2008)

The computational principles underlying the processing of sensory-evoked synaptic inputs are understood only rudimentarily. A critical missing factor is knowledge of the activation patterns of the synaptic inputs to the processing neurons. Here we use well-defined, reproducible skin stimulation to describe the specific signal transformations that occur in different parallel mossy fiber pathways and analyze their representation in the synaptic inputs to cerebellar granule cells. We find that mossy fiber input codes are preserved in the synaptic responses of granule cells, suggesting a coding-specific innervation. The computational consequences of this are that it becomes possible for granule cells to also transmit weak sensory inputs in a graded fashion and to preserve the specific activity patterns of the mossy fibers.

cerebellum | cuneate | lateral reticular nucleus

First-order processing of sensory inputs within the mammalian brain occurs within the spinal cord, brainstem nuclei, and thalamus, as well as in the input layers of specific parts of the cerebral and cerebellar cortices. For example, skin sensory input destined for the cerebellar granule layer can be preprocessed through either the cuneate nucleus pathway (1) or the spinal cord–lateral reticular nucleus (LRN) pathways (2) before being processed further by the granule cells. In the cuneate nucleus, neurons process raw primary afferent input mediated directly from skin receptors, and a set of rather intricate connectivity patterns ensures that the information conveyed through the cuneate neurons represent a synthesized receptive field that have sharp borders (3, 4). Thus, it may be speculated that the purpose of the preprocessing is to present the input layers with sensory information in a form that can be more readily used by downstream neurons, eliminating properties of the skin sensory sheet that are not relevant to the central processing. In contrast, the LRN, another important precerebellar source, receives skin sensory input through neurons of the spinal cord that are involved in the mediation of descending motor commands (5, 6). Although both the cuneate and the LRN are strongly influenced by skin input, they are likely to code the same skin input in different ways because of their differences in convergent synaptic inputs and intrinsic cellular properties.

The understanding of the function of the input layers is more limited, but at least for the cerebellar granule cells, various contrasting theories have been proposed (7–9). Cerebellar granule cells have attracted considerable interest because of their relative simplicity; they receive only about 4 mossy fiber synaptic inputs, each of which evokes strong postsynaptic responses (7, 10). Therefore, actually determining the precise role of each individual synapse in neuronal information processing is feasible, if intracellular recordings and a description of the natural activation patterns in vivo of each synaptic input can be obtained. Here we approach this aim by identifying the specific coding of a given skin input in the cells of the cuneate and the LRN, and then comparing the specific coding patterns with the excitatory postsynaptic potential (EPSP) response patterns in granule cells in whole cell recordings in vivo.

Results

Our main approach was to use electrical skin stimulation to evoke responses in precerebellar neurons and granule cells, and to compare the spike responses of the former with the EPSP responses of the latter (Fig. 1). To properly evaluate sensory responses, we always started by identifying the receptive field of the recorded neuron using manual stimulation (Fig. 1*A*; Fig. S1). For all precerebellar units/granule cells recorded from, the receptive fields were located distally, covering parts of the skin of 1 or 2 adjacent digits, or somewhat more proximally, that is, on the dorsal or ventral part of the paw or the ulnar or radial part of the forearm skin. There was essentially no difference in the size or location of the receptive fields between units of the cuneate and units of the LRN. To illustrate that these units were strongly driven by skin input from restricted receptive fields, the input from the skin was quantified by constructing peristimulus histograms of the manually evoked responses (Fig. S1). The data of these histograms were then used to calculate a response-to-baseline ratio (RBR); see *Materials and Methods*. The RBRs for the center of the receptive field ranged from 15 to 40 for cuneate units and from 3 to 20 for LRN units [mean ± standard deviation, 26 ± 12 (n = 14) and 7.1 ± 3.6 (n = 18), respectively]. The relatively large difference between the 2 groups can be explained by the fact that a subgroup of LRN neurons had, on a relative scale, weak responses to the manual stimulation (RBRs of 3–7) and that even though some LRN units occasionally had equally strong or even stronger responses than the average cuneate unit, the response variability between stimulation trials was substantial for the LRN units, and this variability produced marked reductions in the RBR value. For both the cuneate and LRN units, manual stimulation applied to skin areas just adjacent to the identified border of the receptive field evoked essentially no response (RBR of approximately 1), indicating that the receptive fields were very well localized and had sharp borders.

Receptive fields of central neurons are typically composed of a sensitivity center surrounded by a periphery with weaker, more variable activation (11–13) (Fig. S1). To avoid response variability associated with skin receptor activation (14), we used closely spaced (5–10 mm apart) percutaneous skin needles to deliver electrical shocks within the sensitivity center of the receptive field. Note that although the electrical skin stimulation has the advantage of providing controllable inputs across the population of recorded cells, the responses evoked are not directly translatable to those obtained under more natural forms of synaptic input (7).

Author contributions: H.J. designed research; F.B. and H.J. performed research; F.B. and H.J. analyzed data; and F.B. and H.J. wrote the paper.

The authors declare no conflict of interest.

This article is a PNAS Direct Submission.

[1]To whom correspondence should be addressed. E-mail: henrik.jorntell@med.lu.se.

This article contains supporting information online at www.pnas.org/cgi/content/full/0808428106/DCSupplemental.

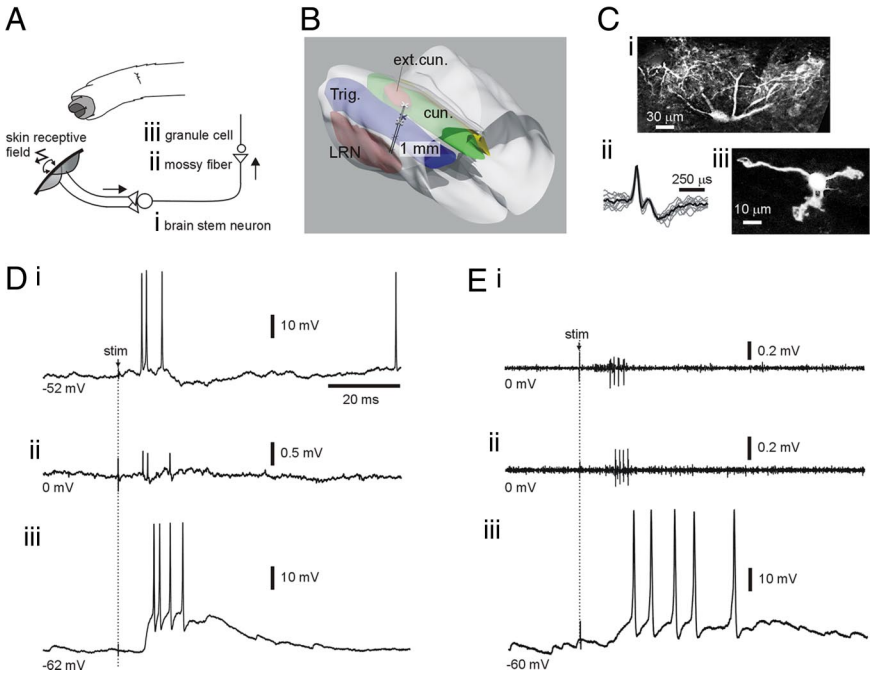

Fig. 1. Experimental setup. (*A*) All recordings were made from structures that mediate skin sensory input from the forelimb to the cerebellum. All units recorded from had an identified receptive field on the distal forelimb. We recorded from precerebellar units in the brainstem (1) and from mossy fibers (2) and granule cells (3) in the cerebellar cortex. The schematic illustrates how these elements are wired together. Note that unipolar brush cells are not part of the circuitry in this part of the cerebellum (28). (*B*) A 3-dimensional reconstruction of the lower brainstem. Precerebellar brainstem neurons were recorded from the cuneate (cun) and LRN. Bar with scale marks indicate the location of one reconstructed electrode track to the LRN. (*C*) Some cuneate (1) granule cells (3) were recorded with neurobiotin in the recording solution and could be morphologically recovered. Mossy fiber terminals were recorded extracellularly (2) and displayed the typical electrophysiological characteristics: a very fast spike (< 0.3 ms), followed by a ''glomerulus'' potential that indicates the synaptic activation of granule cells (16, 29). (*D*) Spike activity evoked by electrical skin stimulation (stim) in a cuneate neuron (1), a mossy fiber terminal (2), and a granule cell (3). (*E*) Spike responses with somewhat longer response latencies (see text) evoked in an LRN cell (1), a mossy fiber terminal (2), and a granule cell (3). Software high-pass filters were applied to the recordings in (1) and (2).

On electrical skin stimulation, brainstem neurons responded with different response onset latency times (latencies). Whereas the cuneate neurons formed a relatively homogenous population in this respect, LRN neurons varied widely and appeared to be distributed along a continuous line on which the longest response latencies were twice as long as the shortest ones. In addition, many (but not all) of the other parameters investigated clearly indicated that the LRN neurons formed an inhomogeneous population with little tendency to form distinct subpopulations. The difference in the response latencies on electrical skin stimulation between cuneate cells (4.92 ± 0.24 ms; $n = 14$) and LRN neurons (10.4 ± 2.8 ms; $n = 18$) was statistically significant ($P < .05$). In addition, the response latencies of the 6 LRN units with the shortest response latency times (7.92 ± 0.95) were statistically significantly different ($P < .05$) from those of the cuneate neurons.

The cuneate response pattern was a stereotyped, 2-component response (Fig. 1*D*). The first component consisted of 2 or 3 spikes discharged at just below 1,000 Hz (870 ± 40 Hz; $n = 14$). The second component consisted of 1 or 2 spikes that appeared after a delay of 4–15 ms relative to the start of the first response component (response latency component 2: 14.3 ± 3.85 ms). Because of these 2 distinct response components, the ratio between the second and first interspike intervals (ISIs) was as high as 6.3 ± 4.1.

''Cuneate'' response patterns also were recorded in 3 mossy fiber terminals (cf. Fig. 1*D*), although the latencies were 1 ms longer because of the conduction time from the brainstem (1). After compensation for this delay, the response latency times for components 1 and 2 (5.94 ± 0.25 ms and 13.4 ± 3.14 ms, respectively; $n = 3$) and the discharge rate in the first component (920 ± 21 Hz) did not differ ($P > .05$) from the corresponding values in cuneate neurons.

The responses recorded from LRN neurons (cf. Fig. 1*E*) were characterized by a large interstimulus variability. The sum of the coefficient of variation (CV) for the latency times of the first 3 spikes was 26% ± 11% ($n = 18$, LRN units responding with 3 or more spikes), statistically significantly different from cuneate neurons (9.2% ± 4.0%). In addition, the ratio between the second and first ISIs in the LRN neurons (1.1 ± 0.10) differed from the much higher value in the cuneate neurons ($P < .01$). Four mossy fiber terminals with similar response latencies (correcting for the 1-ms conduction delay) and properties as the LRN neurons also were recorded.

To analyze the response patterns of synaptic inputs in granule cells, we made intracellular whole cell granule cell recordings ($n = 28$) in the cerebellar C3 zone, which receives a massive mossy fiber input from the forelimb skin through the cuneate and LRN. A projection from the cuneate and LRN to the C3 zone was verified by low-threshold electrical activation of local mossy fiber field potentials and, in some cases, also by activation of EPSPs in the granule cells (Fig. S2).

In some granule cells, electrical skin stimulation evoked synaptic responses at response latencies equal to those of cuneate neurons (6.5 ± 0.50 ms; $n = 11$) when corrected by 1.5 ms to allow for conduction time and synaptic delay. With this correction, the response latencies of the EPSPs in these granule cells (henceforth referred to as type I) did not differ from those in the cuneate neurons ($P > .05$). But the type I granule cells had significantly shorter response latency times than the 6 granule cells with the shortest response latency times within the non–type I group of neurons (8.9 ± 0.45 ms; $P < .05$). As for the

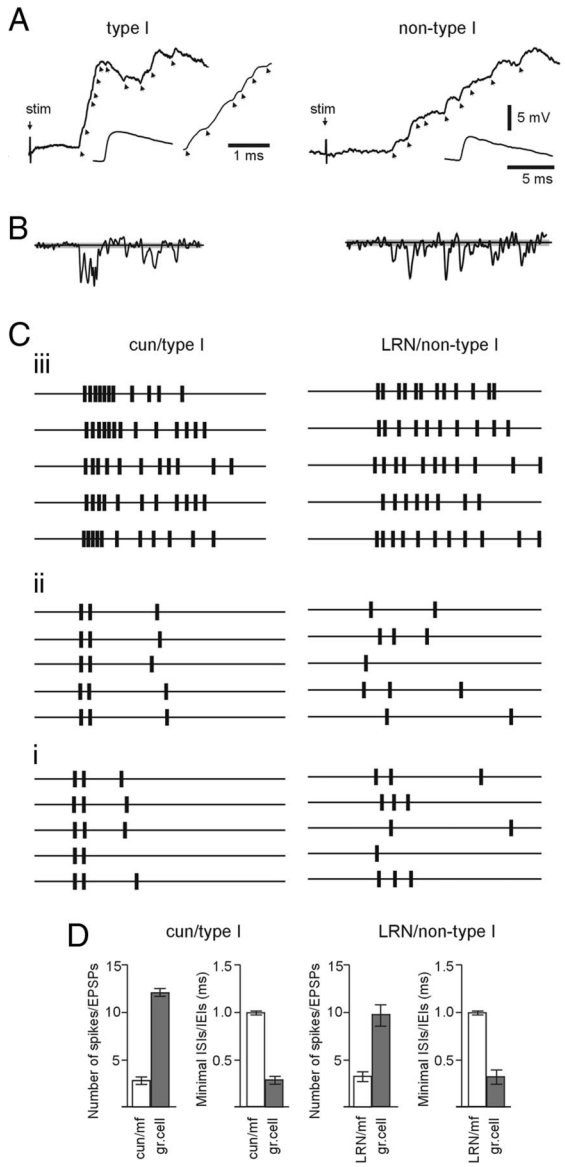

Fig. 2. Sensory-evoked responses in granule cells and precerebellar neurons. (*A*) EPSP responses evoked by electrical skin stimulation in a type I cell (*Left*) and a non–type I granule cell (*Right*), as defined by their response latencies. Insets show averages of the largest spontaneous EPSPs recorded and, for the type I cell, an expansion of the first 2 ms of the response. Arrows indicate starting points of identified EPSPs in the response. The time calibration also applies to (*B*) and (*C*). (*B*) Derivative data of the EPSP responses shown in (*A*). The gray area indicates the standard deviation (SD) of the baseline. Note that the derivative of each identified EPSP exceeded baseline noise by at least 4 SDs. (*C*) Five consecutive traces each of responses evoked in granule cells (3), mossy fiber terminals (2), and brainstem neurons (1) of type I cells (*Left*) and non-type I cells (*Right*). (*D*) Graphs showing the number of evoked spikes and minimal interspike/inter-EPSP intervals. Brainstem neurons and mossy fibers (cun, $n = 17$; LRN, $n = 32$) and EPSPs (granule cells: type I, $n = 11$; other, $n = 17$). Values from left to right: 2.77 ± 0.27, 12.2 ± 0.35, 0.98 ± 0.03 ms, 0.27 ± 0.03 ms, 3.45 ± 0.42, 9.82 ± 0.89, 0.99 ± 0.02 ms, and 0.31 ± 0.05 ms.

precerebellar units, the difference became even larger when the comparison was made with the entire non–type I population of granule cells (11.6 ± 2.5 ms).

The EPSP responses evoked in both type I and non-type I granule cells were composed of a large number of individual elements, and the evoked, compound EPSPs were several-fold larger than the largest spontaneous EPSPs (Fig. 2*A*). Note that

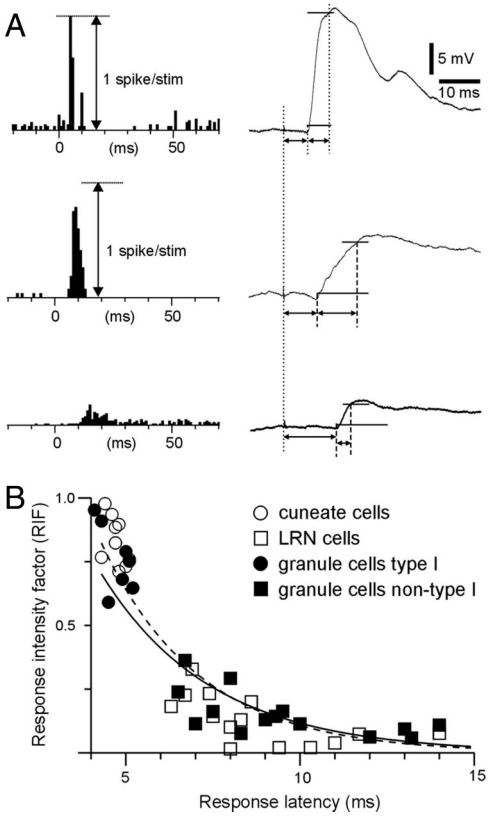

Fig. 3. Relationship between response latency and response intensity. (*A*) Peristimulus histograms of evoked spikes in a cuneate, a fast-responding LRN and a slow-responding LRN unit (*Left*) and averaged EPSP responses of 3 different granule cells with corresponding relative response latencies (*Right*). Dotted lines and arrows indicate measures used for calculating the response latency and the 10%–90% rise time. (*B*) Plot of the RIF against the response onset latency times for brainstem neurons and granule cells of the types indicated. Granule cell latency times were reduced by 1.5 ms to compensate for the conduction and synaptic delays (see text). Curves represent exponential fits for the recorded data (solid line) and the data obtained from the model (dashed line) (see text).

because EPSPs were identified on relatively strict criteria based on the derivative of the voltage trace (Fig. 2*B*), the number of events likely represents an underestimation. Interestingly, the numbers of evoked spikes in terminals and brainstem neurons were lower than the number of EPSPs in granule cells ($P < .001$; Fig. 2*C*) by about a factor of 4, corresponding to the average number of available mossy fiber synapses on granule cells (7, 10) (Fig. 2*C* and *D*). The shortest ISIs/inter-EPSP interval (IEIs) also differed significantly between the presynaptic and postsynaptic elements; no precerebellar neuron/mossy fiber fired at shorter intervals than 0.95 ms, whereas the minimal IEI in granule cells was 0.23 ms (Fig. 2*C*). This indicates that the activity in a single mossy fiber could not possibly account for the EPSP responses of the granule cell.

We also calculated the CVs for the latency times of each of the first 6 evoked EPSPs. This value was 19% ± 1.3% for type I granule cells, compared with 73 ± 42% for non–type I cells ($P < .05$). To some extent, this difference between the 2 populations seemed to parallel the difference in CV for the evoked spikes between cuneate and LRN units (9.2% and 26%, respectively; see above). In addition, as in cuneate neurons, the average EPSP response in type I cells, in contrast to that in non–type I cells, contained a distinct second response component (defined as a voltage increase of at least 2 mV with a 10%–90% rise time of <3 ms; see Fig. 3*A*).

To further evaluate the possibility that granule cells receive their input from specific subsets of precerebellar units, we analyzed the spontaneous activity of these units and compared them with the spontaneous EPSP activity in granule cells. We divided the population of LRN units into 2 distinct groups based on their spontaneous discharge rates. One group discharged at a relatively high, regular rate of 23.3 ± 8.8 Hz (n = 15), and the other fired at only 1.7 ± 0.86 Hz (n = 12). In contrast, all cuneate units had a relatively low and irregular spontaneous firing rate (9.4 ± 4.4 Hz). Interestingly, type I granule cells had spontaneous EPSP rates of 35 ± 7.1 Hz (n = 11), whereas non–type I cells had spontaneous EPSP rates of either 82 ± 29 Hz (n = 11) or 11 ± 2.6 Hz (n = 5). Accordingly, the 3 different spontaneous rates in the precerebellar units matched those of the EPSPs in the corresponding granule cells if multiplied by a factor of 4 (Fig. S3). For both precerebellar units and granule cells, each group had a distribution that was statistically significantly different from that of the other 2 groups with respect to the spontaneous discharge. Note, however, that the 2 separate groups of LRN neurons were not coupled to any specific set of response latencies (Fig. S3). Thus, the variation in spontaneous firing rate provided another means by which the LRN neurons were diversified.

In granule cells, the most intense spike trains/bursts clearly were evoked by EPSP responses that have a large amplitude and fast rise time (7; also see Fig. S4). In addition, the responses of the precerebellar units clearly differed in terms of the intensity of the spike trains evoked by skin stimulation. To further evaluate this relationship, we used a formula for quantifying the response intensity (RIF; see Fig. S5), which measures the peak amplitude versus the rise time/duration of the response in a linear fashion. RIF values for spike responses were based on the average spike response times (plotted as peristimulus histograms; see Fig. 3*A*). For granule cells, the corresponding RIFs were calculated from their average EPSP responses (Fig. 3*A*). Fig. S4 illustrates that EPSP responses with different RIF values resulted in corresponding differences in spike output. When plotted against the response latencies, the time–RIF relationship for precerebellar neurons and granule cell EPSPs could be fitted to a curve by exponential regression [RIF = 2.56*0.73exp(response latency); R2 = 0.73; $P < .05$]. The difference in RIF between type I granule cells and non–type I granule cells was significant (0.76 ±+/-0.13 vs. 0.15 ± 0.09; $P < .001$), as was the difference between cuneate and LRN neurons (0.83 ± 0.09 vs. 0.12 ± 0.10; $P < .001$). In contrast, there was no difference between cuneate neurons and type I granule cells ($P = .27$) or between LRN neurons and non–type I granule cells ($P = .51$).

To analyze the effects of different precerebellar spike patterns on the granule cell EPSP patterns, we used a model of granule cell synaptic integration (10). To test the hypothesis that the response patterns evoked in the granule cells depended on a convergence of mossy fiber input from precerebellar neurons with very similar response patterns, we fed the spike response times evoked at different stimulations in the same precerebellar neuron to all 4 synaptic inputs of the model (Fig. 4*A*). Each of the 4 mossy fiber inputs of the model was assigned a specific EPSP amplitude, which was motivated by results from a previous investigation that indicated a low variability and specific amplitudes for individual mossy fiber synapses in vivo (7). Fig. 4*B* illustrates the EPSP responses modeled from the spiking activity of the 3 precerebellar neurons shown in Fig. 3*A*. Fig. 4*C* illustrates the averages of the modeled EPSP responses and compares them with the recorded granule cell EPSP responses also shown in Fig. 3*A*. A plot of the RIFs of the modeled granule cell responses (based on spike times from 10 cuneate neurons and 20 LRN neurons) against response latencies indicated a similar distribution as for the recorded granule cell responses (exponential regression curve for modeled EPSP responses: y = 3,55*0,70exp(x); R2 = 0.84; $P < .05$) (dashed line in Fig. 3*B*). In contrast, using the model to test the alternative hypothesis that precerebellar neurons that code the skin input with different response patterns resulted in EPSP responses not seen in the granule cell recordings (Fig. 4*D*). For this purpose, we arbitrarily divided the LRN cells into fast responders and slow responders (division line: 10 ms response latency). The modeled granule cell responses from a combination of cuneate and fast LRN or cuneate and slow LRN inputs fell distinctly outside the latency–RIF relationship shown in Fig. 3*C*, because all RIFs were below 0.45 (range, 0.08–0.44), whereas all response latencies were around 5 ms. Because the LRN units formed a continuous population in terms of the distribution of response latency times and response intensities (Fig. 3*B*), with this analysis, it would of course be impossible to precisely determine to what extent LRN units with different response latency times are combined in granule cells. But the fact that the relationship between the response latency and response intensity for granule cell EPSPs was reproduced in the granule cell model when the response times of single precerebellar cells were fed to all 4 mossy fiber inputs of the model (Fig. 3*B*, dashed line) suggests that convergence did not occur between LRN cells with widely different response latency times and response intensities.

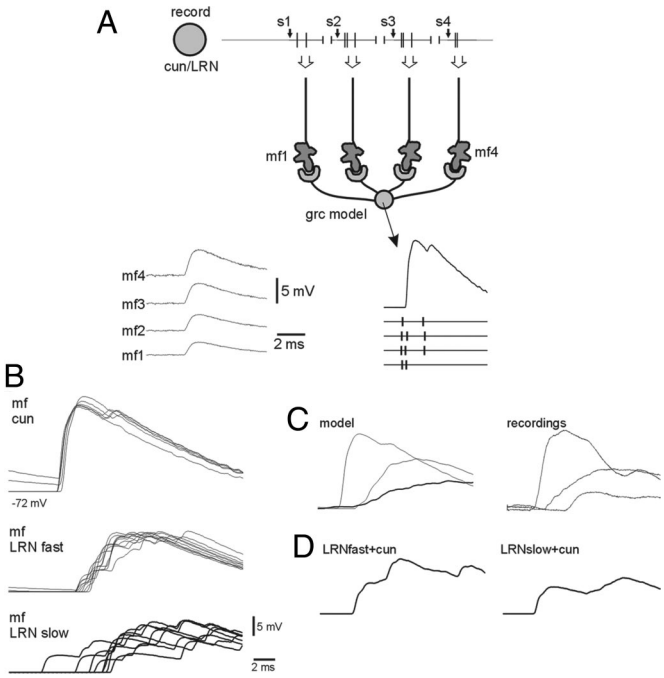

Fig. 4. Modeling of granule cell EPSP responses. (*A*) Experimental setup. The spike patterns recorded in single precerebellar neurons were fed to the mossy fiber inputs of the model. Each mossy fiber input was assigned a specific EPSP amplitude. In each sequence of 4 stimulations (s1–s4), the spike times recorded in the precerebellar unit were used to activate the 4 different mossy fiber inputs of the granule cell model. From this input, the model generated a summated EPSP response. This procedure was repeated for every 4 stimulations, that is, s5–s8, s9–s12, and so on. (*B*) Modeled EPSP responses for spike patterns recorded from a cuneate neuron, a LRN cell with short average response latency (LRN fast) and a LRN cell with long average response latency (LRN slow). (*C*) Comparison of recorded and modeled average EPSP responses. Recorded granule cell responses were from granule cells with fast type I, fast non–type I, and slow non–type I responses. (*D*) Modeled EPSP responses with 2 mossy fibers activated with spike responses of a cuneate neuron and the other 2 mossy fibers activated either from a LRN fast-response unit or a LRN slow- response unit. The calibrations in (*B*) also apply to (*C*) and (*D*).

Discussion

We found that different precerebellar neurons responded to electrical skin stimulation with specific patterns or codes, which

were linked to the specific response latencies as well as to the brainstem nuclei of origin. The specific response patterns found in mossy fibers also were detectable in the EPSP responses of granule cells with corresponding relative response latencies, although the number of underlying events was 3–4 times higher. Furthermore, we found a close relationship between the response latency time and the response intensity for both precerebellar spike responses and granule cell EPSP responses. In addition, the spontaneous spike activity and spontaneous EPSP activity displayed a parallel specificity to response type in precerebellar neurons and granule cells. These findings suggest that most or all mossy fiber inputs to a granule cell code skin input in a similar way. This arrangement provides for new mechanisms of brain sensory processing; it maximizes the probability that weak sensory events are transmitted with high fidelity (Fig. S6) while the function of the input cell as a strong noise-reducing filter is preserved.

Our findings, referred to as the similar coding principle below, indicate that the mossy fibers innervating a granule cell not only carry information from the same modality and receptive field (7), but also seem to code the sensory information in the same way. In contrast, mossy fibers that code the sensory information differently terminate on separate sets of granule cells. The separation of differently coded input is important, because differences in encoding could reflect the signaling of different aspects of the same sensory event. An obvious example of this is the difference between the cuneate and LRN neurons; cuneate neurons are more devoted to the pure sensory aspect, whereas the LRN cells receive their skin input through spinal interneurons mediating descending motor commands to the α motor neurons (5).

A similar coding principle was demonstrated for the mossy fiber input, and sample recordings demonstrated that the spike output code is different in granule cells that receive differentially coded mossy fiber inputs (Fig. S4). Granule cells have been found to be relatively simple spike encoders; that is, they feature a relatively linear and uncomplicated conversion of depolarization level to spike rate (7, 15). Thus, it is a logical consequence that the spike output of the granule cells also can be expected to reflect this coding principle, at least during low-intensity, rate-coded mossy fiber activation, which appears to be the prevailing form of activation under this behavior (16, 17). But during high-intensity mossy fiber bursts, the translation of mossy fiber input to a depolarization level in the granule cell possibly may not be entirely linear; for example, both cuneate and LRN mossy fibers can fire at up to 1,000 Hz during skin stimulation (2, 18), a frequency at which the depression of the synaptic transmission to granule cells is profound (7).

Thus, cerebellar input processing apparently differs from that of the electrosensory system of the weakly electric fish, a model system in which a detailed characterization of sensory processing has been achieved. Here the neural correlates of the fundamental sensory functions of event/feature detection and estimation of a time-varying signal have been ascribed to spike bursts and spike frequency modulations, respectively (19). This feature extraction occurs at the level of the first input cell—the electrosensory pyramidal cell—which uses dendritic processing and regenerative cellular responses to generate a burst output if the primary sensory input contains information about a specific event (20, 21). If the sensory input does not contain such events, but instead carries a lower-frequency, time-varying signal, then the cell does not generate a burst, but rather encodes the input in a more linear fashion (19). Interestingly, in the mammalian skin sensory system, these fundamental features apparently are laid down already at the stage of the primary afferents, with a possible contribution of precerebellar processing in magnifying the feature extraction. The skin information contained in the mossy fiber systems that we evaluated here were composed of both hair follicle afferents and skin tactile afferents (18). Although the primary afferents of both submodalities are excellent tactile event detectors, coded with bursts in the mossy fibers (7, 18), they also function as proprioceptors, and then as rate-coding estimators operating at lower firing frequencies (22, 23).

The similar coding principle is an ideal computational principle for implementing a strong noise-reducing filter (both peripheral receptors and individual integrating neurons are noisy spike-encoders; see ref. 24 for a review) while maximizing the probability that minute sensory events are transmitted as well (Fig. S6). This is an important new aspect of granule cell function, because the capability of fine sensory discrimination, important for tactile discrimination and proprioception, is thought to depend on the detailed timing of just a few spikes (14). Furthermore, in both proprioception (estimation) and tactile detection, information about the pattern of skin strain and indentation is carried by a population of sensory afferents. The primary afferents with receptive fields in the center of the skin strain/indentation are most strongly activated, but the primary afferents with adjacent receptive fields, which are more weakly activated, carry important aspects of the information, making it possible for the brain circuitry to form a richer, more complete picture of the nature of the sensory event. The similar coding principle maximizes the probability that also these weak "fringe" zone events are transmitted (Fig. S6) and at the same time filtered from noise, and thus can ensure that the more central processing units (e.g., Purkinje cells and molecular layer interneurons) receive reliable information about all aspects of the available sensory information.

Our findings regarding granule cell function differ from the conclusions drawn from granule cell recordings in whisker-related areas of the rat (9) and in a vestibular-related system of the mouse (17). It is conceivable that the mossy fiber convergence patterns differ between different functional areas of the cerebellum; for example, the whisker system may function differently from other somatosensory systems, in that they may have the sole function of event detection, not proprioception. Thus, burst activation possibly may be the sole operating mode of these afferents, and the system may have adapted to this arrangement by allowing bursts in single mossy fibers to influence granule cell output (9). In contrast, in the system studied here, it was shown previously that a single mossy fiber will not activate the granule cell spike, not even when activated at 1000 Hz, but spike activation depends on the synchronous activation of 3 or 4 mossy fibers (7). Arenz *et al.* (17) reported that granule cells with rotation-activated EPSC-inputs had very small EPSCs that were not modulated during rotation, even though all of the medium-to-large EPSCs were clearly modulated. They concluded that the nonmodulated EPSCs may represent nonvestibular information (17).

One important difference between the present study and previous in vivo studies of mossy fiber convergence in granule cells is that our conclusions are supported by a systematic (18) and detailed characterization of mossy fiber inputs. Given the wide variety of mossy fiber responses to the same stimulation, such information is crucial to any conclusions on this issue.

Apart from its feature of allowing transmission of weaker sensory inputs in a graded fashion, the similar coding principle also implies that the granule cell spikes consistently represent the same type of information, and that no substantial information convergence occurs among the granule cells. Instead, all integration of sensory information within the system must occur in the downstream Purkinje cells and their afferent inhibitory interneurons. Arguably, this makes sense, because the sensory integration

through these neurons is regulated by synaptic plasticity (25–27) under the control of a feedback signal related to the performance of the movement controlled by the Purkinje cells (26, 27).

Materials and Methods

In decerebrated cats, we made patch clamp recordings from cerebellar granule cells and the cuneate nucleus and extracellular metal electrode recordings from the cuneate and the lateral reticular nuclei, as well as from mossy fiber terminals. Data are given as mean ± standard deviation. For a complete, detailed description of the materials and methods used, see *SI Text*.

ACKNOWLEDGMENTS. This work was supported by SENSOPAC (an Integrated Project funded by the EU under FP6, IST-028056-SENSOPAC), the Swedish Research Council (Projects K2005–04X-14780–03A and K2006–04X-08291–19-3), the Segerfalk Foundation, and the Swedish Medical Society.

1. Cooke JD, Larson B, Oscarsson O, Sjolund B (1971) Organization of afferent connections to cuneocerebellar tract. *Exp Brain Res* 13:359–377.
2. Clendenin M, Ekerot CF, Oscarsson O (1974) The lateral reticular nucleus in the cat, III: Organization of component activated from ipsilateral forelimb tract. *Exp Brain Res* 21:501–513.
3. Bystrzycka E, Nail BS, Rowe M (1977) Inhibition of cuneate neurones: its afferent source and influence on dynamically sensitive ''tactile'' neurones. *J Physiol* 268:251–270.
4. Soto C, Aguilar J, Martin-Cora F, Rivadulla C, Canedo A (2004) Intracuneate mechanisms underlying primary afferent cutaneous processing in anaesthetized cats. *Eur J Neurosci* 19:3006–3016.
5. Alstermark B, Lindstrom S, Lundberg A, Sybirska E (1981) Integration in descending motor pathways controlling the forelimb in the cat, 8: Ascending projection to the lateral reticular nucleus from C3–C4 propriospinal also projecting to forelimb motoneurones. *Exp Brain Res* 42:282–298.
6. Ekerot CF (1990) The lateral reticular nucleus in the cat, VII: Excitatory and inhibitory projection from the ipsilateral forelimb tract (iF tract). *Exp Brain Res* 79:120–128.
7. Jorntell H, Ekerot CF (2006) Properties of somatosensory synaptic integration in cerebellar granule cells in vivo. *J Neurosci* 26:11786–11797.
8. Marr D (1969) A theory of cerebellar cortex. *J Physiol (Lond)* 202:437–470.
9. Rancz EA, *et al.* (2007) High-fidelity transmission of sensory information by single cerebellar mossy fibre boutons. *Nature* 450:1245–1248.
10. Cathala L, Brickley S, Cull-Candy S, Farrant M (2003) Maturation of EPSCs and intrinsic membrane properties enhances precision at a cerebellar synapse. *J Neurosci* 23:6074–6085.
11. Brecht M, Roth A, Sakmann B (2003) Dynamic receptive fields of reconstructed pyramidal cells in layers 3 and 2 of rat somatosensory barrel cortex. *J Physiol* 553(Pt 1):243–265.
12. Ekerot CF, Garwicz M, Schouenborg J (1991) Topography and nociceptive receptive fields of climbing fibres projecting to the cerebellar anterior lobe in the cat. *J Physiol (Lond)* 441:257–274.
13. Manns ID, Sakmann B, Brecht M (2004) Sub- and suprathreshold receptive field properties of pyramidal neurones in layers 5A and 5B of rat somatosensory barrel cortex. *J Physiol* 556(Pt 2):601–622.
14. Johansson RS, Birznieks I (2004) First spikes in ensembles of human tactile afferents code complex spatial fingertip events. *Nat Neurosci* 7:170–177.
15. D'Angelo E, De FG, Rossi P, Taglietti V (1998) Ionic mechanism of electroresponsiveness in cerebellar granule cells implicates the action of a persistent sodium current. *J Neurophysiol* 80:493–503.
16. van Kan PL, Gibson AR, Houk JC (1993) Movement-related inputs to intermediate cerebellum of the monkey. *J Neurophysiol* 69:74–94.
17. Arenz A, Silver RA, Schaefer AT, Margrie TW (2008) The contribution of single synapses to sensory representation in vivo. *Science* 321:977–980.
18. Garwicz M, Jorntell H, Ekerot CF (1998) Cutaneous receptive fields and topography of mossy fibres and climbing fibres projecting to cat cerebellar C3 zone. *J Physiol (Lond)* 512(Pt 1):277–293.
19. Oswald AM, Chacron MJ, Doiron B, Bastian J, Maler L (2004) Parallel processing of sensory input by bursts and isolated spikes. *J Neurosci* 24:4351–4362.
20. Gabbiani F, Metzner W, Wessel R, Koch C (1996) From stimulus encoding to feature extraction in weakly electric fish. *Nature* 384:564–567.
21. Turner RW, Maler L, Deerinck T, Levinson SR, Ellisman MH (1994) TTX-sensitive dendritic sodium channels underlie oscillatory discharge in a vertebrate sensory neuron. *J Neurosci* 14(11 Pt 1):6453–6471.
22. Appenteng K, Lund JP, Seguin JJ (1982) Behavior of cutaneous mechanoreceptors recorded in mandibular division of Gasserian ganglion of the rabbit during movements of lower jaw. *J Neurophysiol* 47:151–166.
23. Edin BB (2004) Quantitative analyses of dynamic strain sensitivity in human skin mechanoreceptors. *J Neurophysiol* 92:3233–3243.
24. Faisal AA, Selen LP, Wolpert DM (2008) Noise in the nervous system. *Nat Rev Neurosci* 9:292–303.
25. Jorntell H, Ekerot CF (2002) Reciprocal bidirectional plasticity of parallel fiber receptive fields in cerebellar Purkinje cells and their afferent interneurons. *Neuron* 34:797–806.
26. Jorntell H, Hansel C (2006) Synaptic memories upside down: Bidirectional plasticity at cerebellar parallel fiber–Purkinje cell synapses. *Neuron* 52:227–238.
27. Ito M (2001) Cerebellar long-term depression: Characterization, signal transduction, and functional roles. *Physiol Rev* 81:1143–1195.
28. Dino MR, Willard FH, Mugnaini E (1999) Distribution of unipolar brush cells and other calretinin immunoreactive components in the mammalian cerebellar cortex. *J Neurocytol* 28:99–123.
29. Walsh JV, Houk JC, Mugnaini E (1974) Identification of unitary potentials in turtle cerebellum and correlations with structures in granular layer. *J Neurophysiol* 37:30–47.